J Solid State Electrochem (2012) 16:2235–2241
DOI 10.1007/s10008-012-1653-3

ORIGINAL PAPER

Functionalization of graphene with Prussian blue and its application for amperometric sensing of H_2O_2

Su-Juan Li · Ji-Min Du · Yun-Feng Shi · Wan-Jun Li · Shui-Ren Liu

Received: 27 September 2011 / Accepted: 9 January 2012 / Published online: 28 January 2012

Abstract As a two-dimensional carbon material with high surface area and conductivity, graphene shows great promise for designing composite nanomaterials to achieve high-performance electrochemical devices. In this work, we prepared graphene-based nanocomposite material by electrochemically depositing Prussian blue (PB) nanoparticles on the surface of graphene. Fourier transform infrared spectra, SEM, and cyclic voltammetry were used to characterize the successful immobilization of PB. Compared with PB films and graphene sheets, the PB–graphene composite films showed the largest current response to the reduction of H_2O_2, probably due to the synergistic effects between graphene sheets and PB nanoparticles. Therefore, a fast and highly sensitive amperometric sensor for H_2O_2 was obtained with a detection sensitivity of 1.6 μA μM^{-1} H_2O_2 per cm^2 and a linear response range of 50~5,000 μM. The detection limit of H_2O_2 was 20 nM at a signal-to-noise ratio of 3. These obtained results are much better than those reported for carbon nanotubes-based amperometric sensors.

Keywords Prussian blue · Graphene · Hydrogen peroxide sensor

Introduction

Graphene, a single layer of carbon atoms in a closely packed honeycomb two-dimensional lattice, has attracted extensive attention because of its unique nanostructure and extraordinary properties, including high conductivity, high surface area, and low manufacturing cost [1, 2]. These unique properties make graphene a promising supporting component for potential applications in the fields of batteries, supercapacitors, nanoelectronics and electrochemical sensors, etc. [3–6]. Recently, numerous investigations have been focused on graphene-based hybrid nanomaterials to achieve the functionalities of graphene, for further expanding the application range and enhancing the performance of graphene-based materials [7, 8]. Toward this objective, many graphene-based nanocomposites such as polymer/graphene, metal/graphene, and metal oxides/graphene have been successfully designed toward applications in technological fields of catalyst and biosensors. For example, Pt or Pt–Ru/graphene nanocomposite have been used as an electrocatalyst for methanol oxidation, showing better electrocatalytic activity than carbon nanotubes (CNTs) and vulcan-supported Pt or Pt–Ru catalyst [9–11]. It is also reported that Au NPs/graphene [12] or MnO_2/graphene oxide [13] nanocomposite materials could be an ideal nonenzymatic sensor for hydrogen peroxide (H_2O_2). Therefore, integration of functional materials on graphene sheets may hold great promise for enhancing the performance of the graphene-based hybrid materials.

Prussian blue (PB) is a kind of attractive inorganic material with well-known electrochromic and electrocatalytical properties. Due to its high activity and selectivity toward the reduction of hydrogen peroxide, PB is usually recognized as an "artificial enzyme peroxidase" and has been extensively utilized in constructing electrochemical sensors based on measuring H_2O_2 [14–17]. However, as pointed out recently by Li et al. [18], there are some problems that restrain the full development of PB-based amperometric sensor: PB films are usually operated in acidic conditions to avoid being decomposed, which is in conflict with near-neutral physiological solutions for biosensing analysis. Besides, PB

S.-J. Li (✉) · J.-M. Du · Y.-F. Shi · W.-J. Li · S.-R. Liu
School of Chemistry and Chemical Engineering, Anyang Normal University,
Anyang 455002, China
e-mail: lisujuan1981@gmail.com

films present lower electrochemical stability, thus resulting in a reduced lifetime of the biosensor. In order to solve these problems, much endeavor has been devoted to searching for novel supports that can improve the sensor's stability and activity. A general solution to the problem is the utilization of CNTs/PB composites due to the enhanced stability of the composite material [19–21]. Nevertheless, when constructing CNTs/PB composites based electrochemical sensors, multistep processes are usually required to prepare in advance, such as purifying CNTs or presynthesizing PB nanoparticles [22]. These complicated processes limit its large-scale application. Therefore, developing new support materials with simple preparation approach to enhance the stability of PB-based amperometric sensor is still greatly demanded.

Of several possibilities for applications of PB, amperometric detection of H_2O_2 is one of the most exciting. Detection of low levels of hydrogen peroxide is important in many areas such as modern medicine, environmental protection, food control, and also a key factor in the development of efficient biosensors, since H_2O_2 is a product of classic reaction catalyzed by oxidase enzymes [23]. By monitoring the electrochemical response of H_2O_2, the concentration of the enzymatic substrate can be obtained due to their proportional relationship.

Inspired by the unique properties of graphene and its electrocatalytic activity toward reduction of H_2O_2, we reason that when it combined with PB nanoparticles, the resultant PB/graphene nanocomposite electrochemical sensor may bear with improved sensitivity in detecting H_2O_2, due to the synergistic effect between graphene and PB nanoparticles. Hence, in this research, we developed a reliable and fast determination method for H_2O_2 based on PB/graphene nanocomposite material. PB nanoparticles were synthesized on the surface of preimmobilized graphene with an electrochemical deposition method to fabricate a PB/graphene-modified glassy carbon electrode (GCE). Fourier transform infrared (FTIR) spectra, scanning electron microscopy (SEM), and cyclic voltammetry were used to characterize the successful immobilization of PB. The results demonstrate that PB nanoparticles immobilized on graphene support exhibit higher stability than PB films directly on GCE surface. The PB/graphene/GCE presents low potential, high sensitivity, and long-term stability towards electrochemical determination of H_2O_2, which is potential for the development of bioelectronic devices and biosensors.

Experimental

Reagents and apparatus

Spectral graphite (about 50 μm; Shanghai Carbon Co., Ltd.) was used for synthesis of graphite oxide (GO) by using the modified Hummers method [4, 24]. The as-synthesized GO was suspended in water to give a brown dispersion, which was subjected to dialysis for 1 week to completely remove residual salts and acids. Exfoliated GO was obtained by ultrasound of the 0.5 wt.% GO dispersion. H_2O_2, iron chloride hexahydrate ($FeCl_3 \cdot 6H_2O$), and potassium ferricyanide ($K_3Fe(CN)_6$) were purchased from the Chemical Reagent Company of Tianjin (China) and was used without further purification. Other reagents were all of analytical grade. All aqueous solutions were prepared with deionized water.

Electrochemical measurements were performed on a CHI 650 electrochemical workstation (Shanghai Chenhua Instrument Company, China). A three-electrode system was employed with a Ag/AgCl (3 mol L^{-1} KCl) electrode as the reference electrode, a platinum foil as the counter electrode, and the PB/graphene/GCE as the working electrode. All experiments were carried out at room temperature (25±1 °C). Cyclic voltammetric experiments were performed with a scan rate of 50 mV s^{-1} unless otherwise stated.

FTIR measurements were obtained with a Bruker IFS-66v/S spectrometer (Germany) with a KBr plate. SEM (Hitachi, S-4800, Japan) images were used to characterize the morphology of synthesized PB/graphene nanocomposite material.

Preparation of the modified electrodes

Prior to the electrode modification, the GC electrodes with a diameter of 3 mm were successively polished with 1.0, 0.3, and 0.05 μm alumina powder, and then ultrasonicated in ethanol and water, each for 3 min. The graphene-modified electrodes were prepared by a reported method of electrochemically reduction of GO precursor [25]. Typically, 6 μL of the GO dispersion (0.5 mg mL^{-1}) was cast onto the GC electrode and then dried in air at room temperature. The electrochemical conversion of GO to graphene was achieved by applying a cathodic potential of −1.5 V on GO/GCE in 20 mM KH_2PO_4 solution for 10 min. Then, the following electrochemical deposition of the PB nanoparticles on graphene was carried out in an aqueous solution of 2.0 mM $K_3Fe(CN)_6$+2.0 mM $FeCl_3 \cdot 6H_2O$+10 mM HCl+0.1 M KCl by the CV method for 20 circles between 0.0 and 1.0 V until a stable cyclic voltammogram was obtained. The prepared PB/graphene/GCE was rinsed with deionized water and then dried in air for the subsequent electrochemical measurements. In a control experiment, PB nanoparticles were prepared on GC electrode by using the same 20 circles in CV as mentioned above.

A 0.1 M phosphate buffer solution (PBS, pH 5.8) was used as supporting electrolyte for the determination of H_2O_2. Before and after every measurement, the PB/graphene/GCE was activated by successive cyclic voltammetric sweeps between −0.2 and 0.4 V at 50 mV s^{-1} in 0.1 M pH 5.8 PBS.

Results and discussion

SEM characterization of synthesized graphene and PB/graphene composite

The morphology of the prepared graphene and PB/graphene composites modified GCE were characterized by SEM in Fig. 1A, B. It is clear that slices of crumpled silk veil waves that were wrinkled and scrolled are observed on graphene surface (Fig. 1A). The section of wrinkled structure is attributed to the π–π interaction within sheets of graphene. It is just this wrinkled nature that renders the graphene sheets stable and beneficial for maintaining a high surface area on the electrode. From the SEM images of PB/graphene composite, some of PB nanoparticles are uniformly spread out on the surface of graphene sheets (Fig. 1B), which guaranteed efficient electrochemical properties of PB/graphene nanocomposites. These results suggest that our electrochemical deposition method we used can effectively produce homogeneous high-loading PB nanoparticles supported on graphene sheets.

FTIR spectra of PB/graphene composite

FTIR spectra of the prepared PB/graphene composite film are shown in Fig. 2. Meanwhile, the FTIR spectra of GO were also displayed. Curve a shows the pure GO; the bands around 976, 1,056, 1,226, 1,276, 1,384, 1,580, and 1,727 cm^{-1} are attributed to the oxygen-containing functional groups on GO [25, 26], while the band at ca. 1,619 cm^{-1} could be due to the O–H stretching deformation vibration of intercalated water. After the reduction and then modification with PB nanoparticles, the FTIR adsorption bands of oxygen functionalities decrease significantly and even disappear (curve b), which confirmed the successful conversion of GO into graphene. Besides, a new strong absorption band at 2,100 cm^{-1} is attributed to the C=N stretching vibrations of PB [27]. Thus, these are the indicators that PB had been assembled on the surface of graphene through electrochemical deposition method.

Cyclic voltammetric behavior of the PB/graphene/GCE

Cyclic voltammogram of the PB/graphene/GCE in a 0.5-M KCl aqueous solution was carried out at a scan rate of 50 mV s^{-1}. As shown in Fig. 3, a pair of peaks located at 0.254/0.215 V (vs. Ag/AgCl) corresponding to the reversible conversion of PB to Prussian white is observed. The potential separation of the redox peaks is only 39 mV, which is very close to the theoretical value, indicating that fast charge transfer occurs in the modified PB/graphene composite. This phenomenon could be ascribed to the highly electrical conductivity of graphene. The effect of the potential scan rate on the reduction current of PB was investigated in the range of 5 to 1,000 mV s^{-1}. A linear relationship between the peak currents and the scan rates from 5 to 30 mV s^{-1} is observed (inset A), indicating that the present electrochemical reactions are a surface-controlled process. At higher scan rates from 40 to 1,000 mV s^{-1}, the peak currents are found proportional to the square root of the scan rate (inset B), suggesting that the reaction kinetics change from a surface process to a diffusion controlled process. These results are consistent with those reported previously [14, 16, 28].

The stability of the PB/graphene-modified electrode was verified by investigating its cyclic electrochemical behavior in a blank solution of 0.5 mol L^{-1} KCl solution at a potential scan range of 0~1.2 V. As can be observed in Fig. 4A, PB/graphene/GCE shows the typical redox characteristics of PB; apart from the redox pair at ca. 0.2 V corresponding to the conversion of PB to Prussian white, another redox pair at 0.974/0.857 V corresponding to the reversible conversion of PB to Berlin green is observed. After successive scans in the first 30 cycles, it is clear from Fig. 4A that no expressive changes or current decreases are observed in the CV profiles of the PB/graphene-modified electrode, indicating that this PB/graphene composite presents high stability for both the transition between PB and Prussian white and between PB and Berlin green. Compared with PB-modified electrode as Fig. 4B demonstrated, the stability of PB electrochemically deposited on graphene sheet is greatly enhanced.

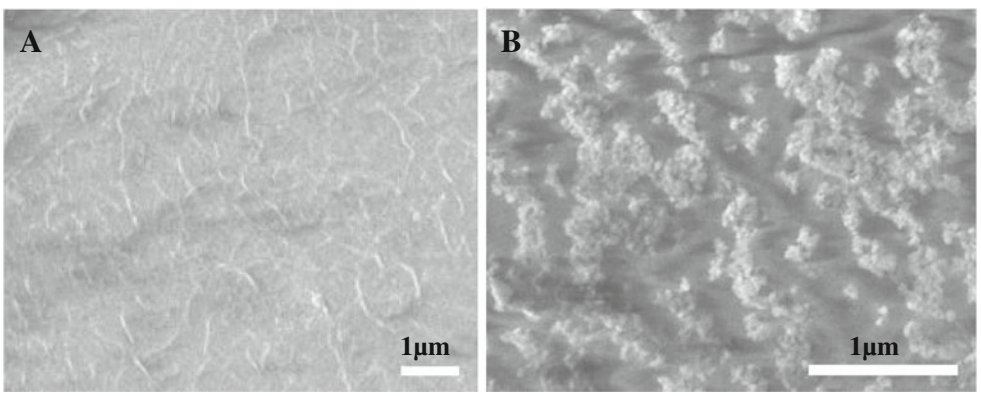

Fig. 1 SEM images of graphene (**A**) and PB/graphene composite (**B**)

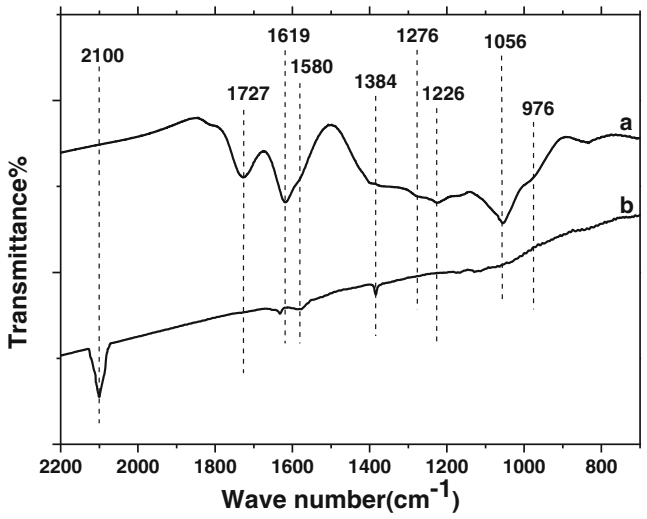

Fig. 2 FTIR spectra of GO (**a**) and PB/graphene composite film (**b**)

Therefore, it is reasonable to conclude that the support of graphene not only maintains the good electrochemical activity of PB but also protect the structure of PB to be not damaged by the intercalation/deintercalation of potassium cations, which means that the present PB/graphene composite is an ideal material for constructing a stable sensor devices.

Electrocatalytic reduction of H_2O_2 at the PB/graphene-modified electrode

In this section, we investigated the electrocatalytic behavior of the PB/graphene nanocomposite on GC electrode toward the reduction of H_2O_2. To distinguish the contribution of individual modified components and the potential synergistic effects among them, control experiments on the bare GCE, graphene/GCE, and PB/GCE were also carried out. Figure 5A–C shows the voltammograms resulting from the bare GCE, graphene/GCE, and PB/GCE in 0.1 M PBS without (black curve) and with 5 mM H_2O_2 (red curve) addition. As can be observed, there is no electrocatalytic activity of the bare GCE toward the reduction of H_2O_2. However, in terms of graphene/GCE and PB/GCE, with the addition of 5 mM H_2O_2, an obvious increased reduction current is observed, indicating that both graphene and PB show electrocatalytic activity toward H_2O_2, which is in accordance with reports of literature. Besides, the onset potential of PB/GCE for electrochemically reduction of H_2O_2 is found at 0.21 V (vs. Ag/AgCl). When the two electrocatalysts are integrated together to form PB/graphene nanocomposite film modified electrode, a remarkable reduction current, which is the largest among all of the electrode, can be observed from the cyclic voltammograms presented in Fig. 5D, recorded in a PBS aqueous solution containing 5 mM H_2O_2. Therefore, the synergistic effects are estimated to occur between graphene and PB nanoparticles. The electrochemical reduction of hydrogen peroxide on the PB/graphene/GCE starts at 0.25 V (vs. Ag/AgCl), which is more positive than the onset potential of PB/GCE. This 40-mV positive shift of the onset potential for the reduction of H_2O_2 on the PB/graphene nanocomposite demonstrates that introduction of graphene support enhances the electrocatalytic activity of the loaded PB nanoparticles. In this process, graphene in the composite films improves the electronic and potassium ionic transport capacity, and the PB nanoparticles act as an electron mediator between the graphene and the hydrogen peroxide in solution.

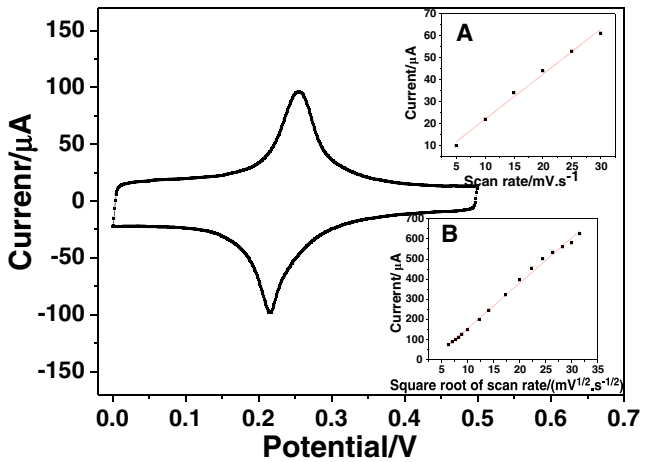

Fig. 3 Cyclic voltammograms of the PB–graphene/GCE in 0.5 M KCl solution at a scan rate of 50 mV s^{-1}. *Inset*: plot of the reduction peak current at 0.215 V vs. the scan rate in the range of 5 to 30 mV s^{-1} (*A*); plot of the peak current at 0.215 V vs. the square root of scan rate in the range of 40 to 1,000 mV s^{-1} (*B*)

Based on the results discussed above, the working potential for the amperometric sensing of H_2O_2 was optimized in the potential range of 0.3 to −0.3 V. Figure 6 shows the amperometric response curves of PB/graphene/GCE at different detection potentials ranging from 0.3 V to −0.3 V (vs. Ag/AgCl) in 2-mM H_2O_2 solutions. Obviously, the reduction currents increase with negative shift of detection potential, and reach a plateau at a potential of −0.2 V as displayed in inset of Fig. 6. Therefore, the working potential for the amperometric H_2O_2 sensor was defined as −0.2 V to ensure enough sensitivity and lower background current.

Figure 7 shows typical amperometric response of the PB/graphene composite film electrode to successive addition of H_2O_2 in pH 5.8 PBS at −0.2 V. For comparison, the responses of PB/GCE, graphene/GCE, and a bare GC electrode under the same conditions were also displayed. Obviously, with the addition of H_2O_2, a stable and increasing amperometric response could be seen on the three modified electrodes, while this phenomenon is not observed at the bare GC electrode. These results are consistent with that obtained from cyclic voltammograms. Compared with the three modified electrode, it can be observed that the response of PB/graphene composite film electrode is the largest,

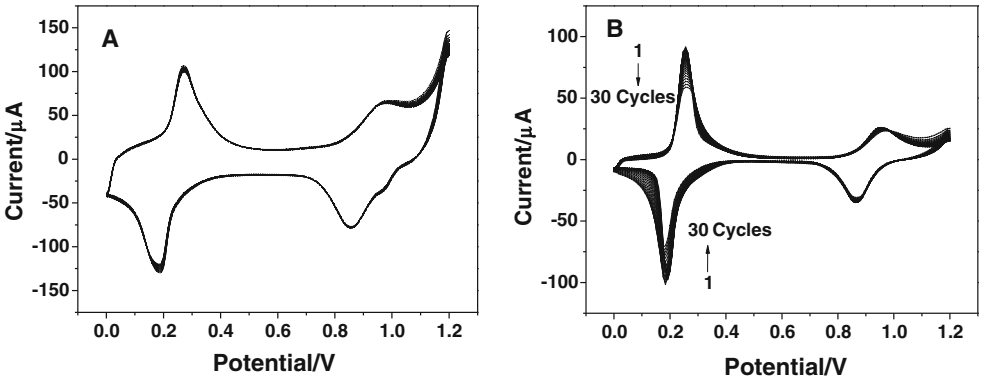

Fig. 4 Cyclic voltammograms of the PB–graphene/GCE (**A**) and PB/GCE (**B**) in 0.5 M KCl solution at a scan rate of 50 mV s^{-1} (30 first cycles)

presenting a current of 4.21 μA with 50 μM H_2O_2 addition. The PB/GCE and graphene/GCE only yields a current of 1.79 and 1.27 μA upon addition of 50 μM H_2O_2. Adding the current of PB/GCE and graphene/GCE together, it is found that this value (3.06 μA) is still smaller than that of PB/graphene composite electrode (4.21 μA). This further indicates that a synergistic effect between graphene and PB nanoparticles occurs toward the electrochemical reduction of H_2O_2. The calibration curves obtained from the three modified electrodes are displayed in Fig. 8. The resultant PB/GCE shows a narrow linear response range (50~950 μM), with further increasing of H_2O_2 concentration, the current response keeps constant and even lowers due to the instability of PB films. Regarding the PB/graphene/GCE, the linear range spans the concentration of H_2O_2 from 50 μM to 5 mM (R=0.9955) with linear equation of I (in microamperes)=8.2098+0.0552C (in micromolars), and the detection limit is 0.02 μM (S/N=3), which is lower than those at PB/multiwalled carbon nanotubes (MCNT)-modified Au electrode (0.023 μM) [27], CNTs/chitosan-modified electrode (10.3 μM) [28], chitosan/multiwalled carbon nanotubes/Hb/AgNPs/GCE (0.347 μM) [29], CNT/AuNPs/PB (3.36 μM) [30], chemically reduced graphene oxide based sensors (0.05 μM) [26], graphene/Au NPs/GCE (0.44 μM, −0.2 V vs. Ag/AgCl) [12], PB/ordered mesoporous carbon composite-based sensor (1 μM) [31], etc. In addition, the sensitivity of the sensor (obtained from the slope of the linear part of the calibration curve) is 1.6 μA μM^{-1} H_2O_2 per cm^2, which is much higher than that reported at PB/MCNT-modified Au electrode (0.856 μA μM^{-1} cm^{-2}). Thus, the present H_2O_2 sensor based on the PB/graphene-based

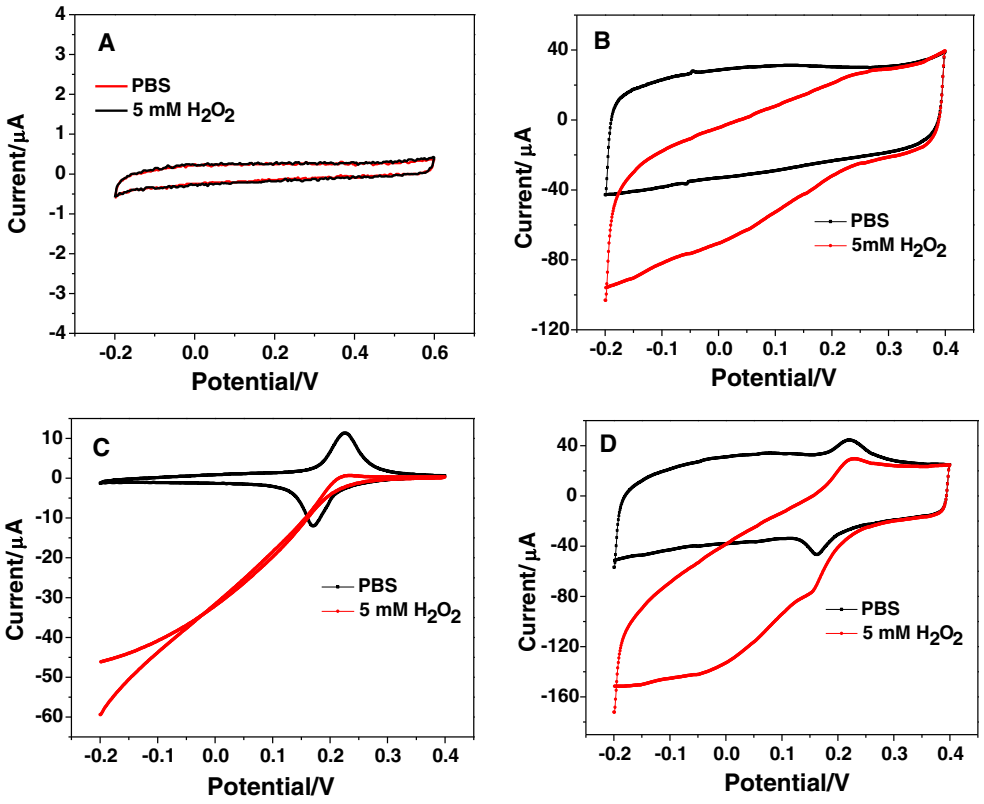

Fig. 5 Cyclic voltammograms of the bare GCE (**A**), graphene/GCE (**B**), PB/GCE (**C**), and PB/graphene/GCE (**D**) in 0.1 M PBS (pH 5.8) without (*black curve*) and with (*red curve*) 5 mM H_2O_2 at a scan rate of 50 mV s^{-1}

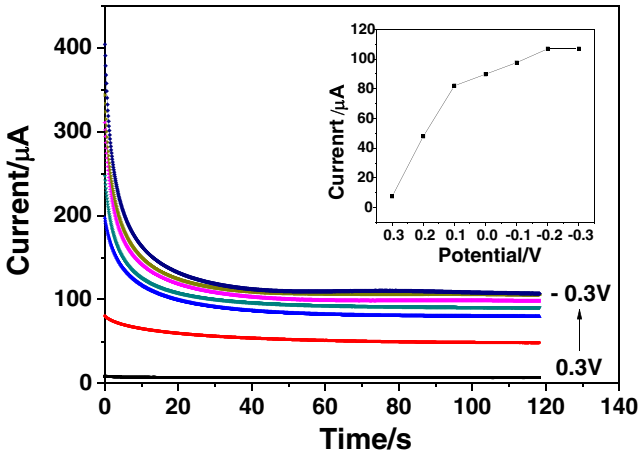

Fig. 6 Current traces of 2 mM H_2O_2 recorded at PB/graphene/GCE, the *inset figure* is the relationship of the amperometric current with detection potentials

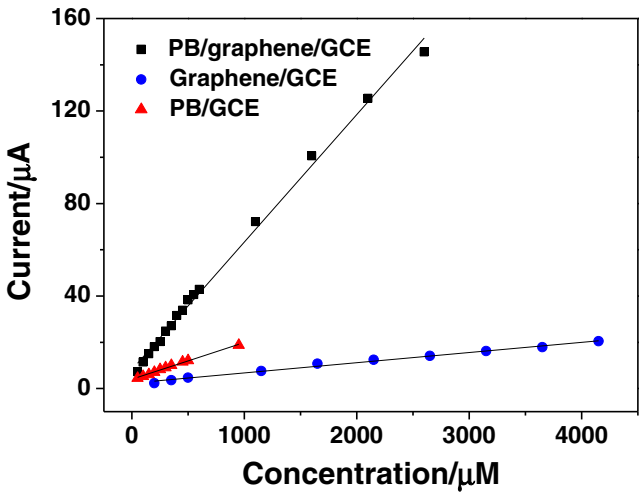

Fig. 8 Calibration curves for H_2O_2 detection at the PB/graphene/GCE, PB/GCE, and graphene/GCE in PBS (pH 5.8)

hybrid material is fast, sensitive, and efficient. It demonstrates that using graphene and some inorganic or metal nanoparticles holds great potentials for constructing biosensors and other bioelectronic devices.

Interferences

The possible interference of some inorganic ions and organic compounds, which might coexist with H_2O_2 in real samples, was investigated with the method of amperometric detection of 50 μM H_2O_2. The result showed that 500-fold of Cl^-, SO_4^-, CO_3^{2-}, NO_3^-, and citric acid did not cause significant interference with deviations below 5%, indicating that these species did not affect the determination of H_2O_2. Ten-fold of glucose, creatinine, trioxypurine, dopamine, uric acid, tyrosine, serine, glycin, lysine did not interfere with the oxidation signal of 50 μM H_2O_2. However, fivefold of Cu^{2+} and Fe^{3+} cause a signal (peak current of H_2O_2) change of about 8.6% and 10.2%, respectively. The possible reason is the catalytic ability of Cu^{2+} and Fe^{3+} to the electrocatalytic reduction of H_2O_2. Therefore, when the two cations are present, a separation procedure is required before determination.

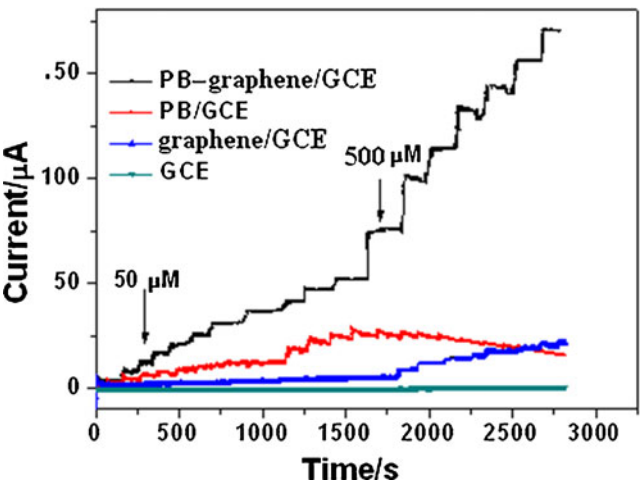

Fig. 7 Current traces recorded at the PB/graphene/GCE, PB/GCE, graphene/GCE, and the bare GC electrode. Steps represent the responses of the electrodes to the successive addition of 50, 500 μM H_2O_2 to the PBS (pH 5.8) solution

Reproducibility and stability

Here, the reproducibility and stability of the PB/graphene composite-modified GC electrodes were investigated by measuring the current responses of the electrode upon addition of 50 μM H_2O_2 in PBS. The average relative standard deviation (RSD) of the sensor response to 50 μM H_2O_2 was 4.8% for ten successive measurements. In a series of eight sensors named PB/graphene composite prepared in the same way, an RSD of 5.6% was obtained, indicating an excellent reproducibility of this sensor. The prepared electrode was stored at room temperature. In order to investigate the stability of the sensor, the current response to 50 μM H_2O_2 was recorded every 5 days. It was found that the current could retain 90.5% of its original signal after a month storage, which showed a long-term stability.

Conclusions

In summary, the PB/graphene nanocomposite film has been successfully deposited on glassy carbon electrode with an electrochemical deposition method. The as-prepared PB/graphene/GCE exhibited a high electrocatalytic activity for the H_2O_2 detection, showing a high sensitivity, a low limit detection, and a wide linear range. The synergetic effect

between PB and graphene occurred, which combined the high catalytic nature of PB with the large surface area of graphene. Therefore, the PB/graphene nanocomposite film holds the promise for applications in other fields including bioelectronics devices, electrochromic displays, nonenzymatic sensor, biofuel cells, and so on.

Acknowledgment This work was supported by the Grants from the Natural Science Foundation of China (No 21105002), Anyang Technology Research Program (208), and the Innovative Foundation for the College students of Anyang Normal University (ASCX/2011-Z12).

References

1. Shao YY, Wang J, Wu H, Liu J, Aksay IA, Lin YH (2010) Electroanalysis 22:1027–1036
2. Chen D, Tang LH, Li JH (2010) Chem Soc Rev 39:3157–3180
3. Hou S, Kasner ML, Su S, Patel K, Cuellari R (2010) J Phys Chem C 114:14915–14921
4. Kovtyukhova NI, Ollivier PJ, Martin BR, Mallouk TE, Chizhik SA, Buzaneva EV, Gorchinskiy AD (1999) Chem Mater 11:771–778
5. Titov AV, Kral P, Pearson R (2009) ACS Nano 4:229–234
6. Kang X, Wang J, Wu H, Liu J, Aksay IA, Lin Y (2010) Talanta 81:754–759
7. Hu Y, Jin J, Wu P, Zhang H, Cai C (2010) Electrochim Acta 56:491–500
8. Wang C, Zhang L, Guo Z, Xu J, Wang H, Zhai K, Zhuo X (2010) Microchim Acta 169:1–6
9. Zhou YG, Chen JJ, Wang FB, Sheng ZH, Xia XH (2010) Chem Commun 46:5951–5953
10. Bong S, Kim YR, Kim I, Woo S, Uhm S, Lee J, Kim H (2010) Electrochem Commun 12:129–131
11. Liu S, Wang J, Zeng J, Ou J, Li Z, Liu X, Yang S (2010) J Power Sourc 195:4628–4633
12. Fang Y, Guo S, Zhu C, Zhai Y, Wang E (2010) Langmuir 26:11277–11282
13. Li L, Du Z, Liu S, Hao Q, Wang Y, Li Q, Wang T (2010) Talanta 82:1637–1641
14. Nossol E, Zarbin AJG (2009) Adv Funct Mater 19:1–7
15. Yu H, Sheng QL, Li L, Zheng JB (2007) J Electroanal Chem 606:55–62
16. Li J, Qiu JD, Xu JJ, Chen HY, Xia XH (2007) Adv Funct Mater 17:1574–1580
17. Xian Y, Hu Y, Liu F, Xian Y, Feng L, Jin L (2007) Biosens Bioelectron 22:2827–2833
18. Li Z, Chen J, Li W, Chen K, Nie L, Yao S (2007) J Electroanal Chem 603:59–66
19. Zhai J, Zhai Y, Wen D, Dong S (2009) Electroanalysis 21:2207–2212
20. Zhang W, Wang L, Zhang N, Wang G, Fang B (2009) Electroanalysis 21:2325–2330
21. Zhang Y, Wen Y, Liu Y, Li D, Li J (2004) Electrochem Commun 6:1180–1184
22. Cao L, Liu Y, Zhang B, Lu L (2010) Appl Mater Interf 2:2339–2346
23. Itaya K, Ataka T, Toshima S (1982) J Am Chem Soc 104:4767
24. Hummers WS, Offeman RE (1958) J Am Chem Soc 80:1339–1339
25. Guo HL, Wang XF, Qian QY, Wang FB, Xia XH (2009) ACS Nano 3:2653–2659
26. Zhou M, Zhai Y, Dong S (2009) Anal Chem 81:5603–5613
27. Du D, Wang M, Qin Y, Lin Y (2010) J Mater Chem 20:1532–1537
28. Qian L, Yang X (2006) Talanta 68:721–727
29. Li Y, Li Y, Yang Y (2011) J Solid State Electrochem. doi:10.1007/s10008-011-1503-8
30. Li MY, Zhao GQ, Yue ZL, Huang SS (2009) Microchim Acta 167:167–172
31. Bai J, Qi B, Ndamanisha JC, Guo LP (2009) Microporous Mesoporous Mater 119:193–199